Journal of Hazardous Materials 176 (2010) 473–480

Contents lists available at ScienceDirect

Journal of Hazardous Materials

journal homepage: www.elsevier.com/locate/jhazmat

Impact of ultrasonic power density on elution of super heavy oil and its biomarkers from aging soils using Triton X-100 micellar solution

Xin Sui[a,b], Guodong Ji[a,*]

[a] Key Laboratory of Water and Sediment Sciences, Ministry of Education, Department of Environmental Engineering, Peking University, Beijing 100871, China
[b] Department of City Planning and Design, School of Architecture and the Built Environment, Royal Institute of Technology, Stockholm SE-10044, Sweden

ARTICLE INFO

Article history:
Received 18 August 2009
Received in revised form 8 November 2009
Accepted 9 November 2009
Available online 13 November 2009

Keywords:
Ultrasonic power density
Triton X-100 micellar solution
Aging soils
Super heavy oil
Biomarker

ABSTRACT

An ultrasound-enhanced elution system employing Triton X-100 solutions was used for remedying aging soils contaminated with super heavy oil. The effect of varying the ultrasonic power density on the elution of the oil and three characteristic biomarkers was analyzed using GC/MS and FTRS. The oil and biomarkers remaining in treated soils decreased as a similar first-order function of increasing ultrasonic power density. Elution of the three biomarkers in the absence of ultrasound was closely related to carbon numbers in the marker: smaller molecules were more readily eluted. This trend was reversed upon application of ultrasound at higher power densities, with improved elution of molecules containing a greater carbon numbers. The two ratios, both 22*S*/(22*S* + 22*R*) of C_{26-34} 17α 25-norhopanes and 20*S*/(20*S* + 20*R*) of C_{26-28} triaromatic steroids, in treated soils decreased with increasing power density from 20 to 100 W L^{-1}. The results of SEM, FTRS, XRD, and energy spectroscopy experiments indicated that the mineral and chemical compositions of soils eluted at power densities greater than 60 W L^{-1} closely resembled clean soils.

1. Introduction

Super heavy oil refers to crude oil with a viscosity of more than 10^5 mPa s in the natural condition. It accounts for approximately 30% of the total crude oil worldwide, and will be an important energy source in the 21st century [1–3]. Inevitably, super heavy oil will enter the environment during oil drilling, extraction, and transportation. Contamination with super heavy oil alters the physical and chemical properties of soils. The presence of toxic polycyclic aromatic hydrocarbons in soil causes great harm to crops and other vegetation and threatens human health as the compounds migrate through the food-chain [4].

Super heavy oil is primarily composed of hydrophobic organic compounds (HOCs). Numerous physical, chemical, and biological remediation technologies such as soil vapor extraction, ex situ chemical leaching, and biological remediation have been developed in recent years to eliminate HOCs from contaminated soils [5,6]. However, poor bioavailability and the presence of volatile organic compounds make it difficult to treat polluted soils effectively [7].

Earlier studies demonstrated that elution using surfactant solutions was a feasible and cost-effective method for treating contaminated soils, and the technique has been extensively studied [6,8]. Anionic surfactant solutions are popular in these studies due to their good solution properties [9]. However, the critical micelle concentration (CMC) of anionic surfactants is usually large and they frequently undergo complexation reactions with Ca^{2+} and Mg^{2+} to produce insoluble sediments, reducing their effectiveness. Triton X-100, as a kind of non-ionic surfactant, possesses the advantage of a small CMC, does not form soaps with Ca^{2+} and Mg^{2+} [9–11], and is typically effective in solubilizing hydrocarbons [12,13]. It has thus become the subject of international interest in the field of HOC-contaminated soil remediation.

Stirring has been used to improve the effectiveness of traditional surfactant elution methods, despite the marginal benefit [6,14]. Earlier studies suggested that besides stirring, the application of ultrasound could significantly increase the efficacy of surfactants in eluting PAHs and diesel fuel [15–18]. When 20 kHz ultrasound was applied for 30 min at a power level of 750 W L^{-1}, Kamalavathany [19] obtained a 65% increase in the average elution of 12 PAHs using a 10 g L^{-1} solution of Triton X-100. Mason et al. [20] obtained a 70% increase in the amount of DDT and PCBs removed when ultrasound was applied for 20 min at a frequency of 20 kHz and a volume power density of 500 W L^{-1}. Feng and Aldrich [14] reported that treatment with 30 kHz ultrasound for 30 min at power densities of 20–100 W cm^{-2} improved the elution of diesel fuel from soils when using sodium dodecyl sulfate (SDS) as the surfactant. The available literature has focused on the impact of ultrasound at high power density on the elution of diesel fuel, light oil, and PAHs, and there have been no reports concerning the effects of ultrasound at low power density on the remediation of soils contaminated with super heavy oil.

* Corresponding author. Tel.: +86 1062765592x87; fax: +86 1062756526.
E-mail address: jiguodong@iee.pku.edu.cn (G. Ji).

0304-3894/$ – see front matter © 2009 Elsevier B.V. All rights reserved.
doi:10.1016/j.jhazmat.2009.11.053

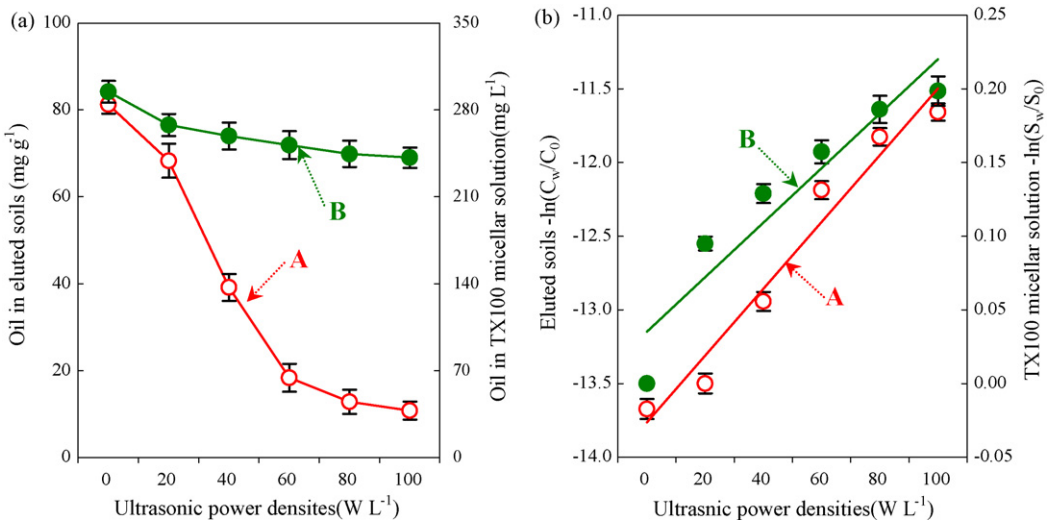

Fig. 1. Concentrations of super heavy oil in eluted soils and Triton X-100 micellar solution. (a: Concentration curve; b: first-order curve). (A: Eluted soils; B: Triton X-100 micellar solution).

We therefore examined the impact of low power density ultrasound (from 0 to 100 W L^{-1}) on the elution of super heavy oil and the three associated biomarkers C_{26-34} 17α 25-norhopanes, C_{26-28} triaromatic steroid (TAS), and C_{27-29} methyl triaromatic steroid (MTAS) from aging soils contaminated with super heavy (AOCS) using Triton X-100 micellar solution. In addition, we investigated the mineral and chemical composition of the eluted soils and the surface characteristics of the AOCS, eluted soils, and suspended solids.

2. Materials and methods

2.1. Preparation of the AOCS

The AOCS was prepared by mixing clean soil and super heavy oil in the laboratory. Clean soil was collected from a surface layer of 0–25 cm depth in an open zone of the Haidian District, Beijing, P.R.C. after removal of surface weeds. The samples were air-dried for one week and debris was removed using a 20-mesh sieve. The organic matter content of the clean soils was 2.7% with a cation exchange capacity of 182 mmol kg^{-1}, and a pH of 6.49. The fraction of particles less than 200 μm in size was 99.5% and the fraction less than 100 μm in size was 96%. Super heavy oil was collected from the Liaohe oil field in China with a viscosity of 8.8×10^5 mPa s at 55 °C and a density of 1.020 g cm^{-1} containing 42% asphalt, and 14% colloid, 28% saturated hydrocarbons, 16% aromatic hydrocarbons. The AOCS was prepared according to the method of Urum et al. [21]. A 3 kg sample of super heavy oil was heated and dissolved in chloroform. The solution was stirred and 27 kg of clean soil was added with continued heating to ensure complete evaporation of the chloroform. The contaminated soil was stored in a ventilated cabinet for approximately 16 h and then aged in a 50 °C oven for 72 h. As measured, the oil concentration of the AOCS was 93.6 mg g^{-1}. Then, the prepared AOCS was stored in beakers at 5 °C.

2.2. Test procedures

The ultrasound-enhanced elution system used in this study included a reactor, a gravity separator, and an automatic controller. The reactor consisted of a cylindrical steel container with a bottom diameter of 100 mm and an effective volume of 3 L, equipped with an ultrasound generator, a stirrer, and a temperature control device. Elution involved mixing 100 g the AOCS with 100 mL of 1.5 g L^{-1} Triton X-100 solution at a mass and volume ratio of 1:10 and placing the mixture in the reactor. The elution parameters were optimized in a previous study [8] and included a temperature of 70 °C, an ultrasonic frequency of 28 kHz, a sonication time of 18 min, a stirring speed of 180 rpm, and an elution time of 30 min. The ultrasound volume power density was adjusted to 0, 20, 40, 60, 80, or 100 W L^{-1} (corresponding to area power densities of 0, 0.255, 0.510, 0.764, 1.019, or 1.274 W cm^{-2}). Three samples were treated in parallel at each power density level. At the conclusion of each trial, the contents of the reactor were discharged into the gravity separator and allowed to settle for 24 h to obtain complete separation of the liquid, solid, and oil phases. The eluent, oil layer, and eluted soil layer were individually collected from the gravity separator for analysis.

2.3. Analytical methods

The concentrations of super heavy oil in the eluent and soil were measured using UV spectrophotometry at a wavelength of 254 nm (SPECORD200, Germany, Analytik Jena AG). For additional information about, see reference [22]. The saturated and aromatic hydrocarbon biomarkers were first extracted using a Soxhlet extractor to obtain non-asphalt compounds, then separated by neutral alumina and silica gel into saturated hydrocarbons, aromatic hydrocarbons, and colloids. The saturated and aromatic hydrocarbons were qualitative analyzed and quantified using GC/MS by sampling 1 μL of a methylene chloride extract. The analysis was performed using a helium flow rate of 1 mL min^{-1} and a MS scan range of 50–600 amu. The temperature program of the GC/MS consisted of holding at 50 °C for 2 min, ramping to 170 °C at a rate of 6 °C min^{-1}, holding at 170 °C for 3 min, ramping to the final temperature of 300 °C at a rate of 2 °C min^{-1}, and holding at 300 °C for 20 min. The compounds 1,2,3,4-tetradeutero cholestane and 1,2,3,4,5,6,7,8-octadeutero cholestane were selected as internal standards [23,24]. The concentrations of the biomarkers in the AOCS and eluted soils were determined by comparison to the two internal standards. The soil particle sizes were measured using a laser particle size analyzer (Malvern 2000, Malvern Instruments Ltd., UK). The surface morphology and energy spectra of the soil particles were analyzed using environmental scanning electron microscopy (SEM, Quanta 200FEG, FEI Company, USA). Organic functional groups were identified using FT-Raman spectroscopy (Raman950/Magna-IR750, Nicolet Com-

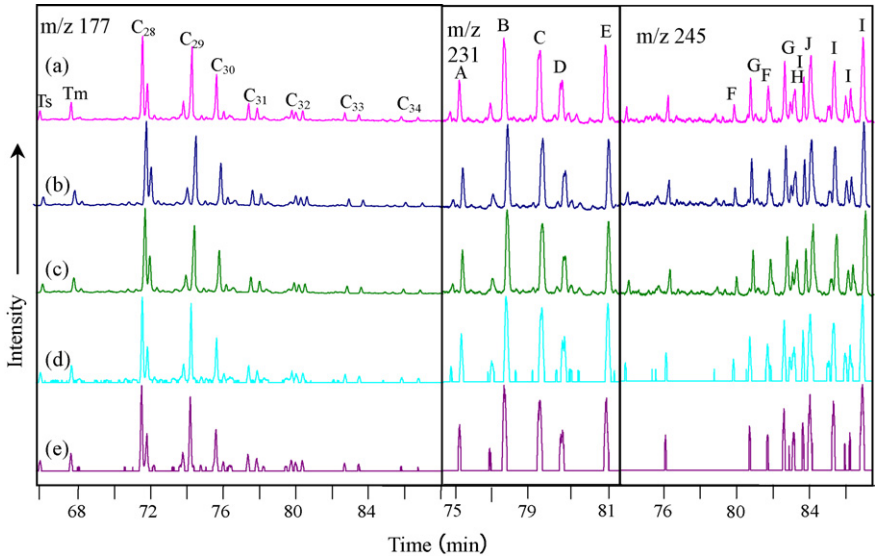

Fig. 2. Abundance of residual 17α 25-norhopanes, TAS and MTAS in the AOCS and eluted soils. (a: AOCS; b: soils treated using 0 W L^{-1}; c: soils treated using 20 W L^{-1}; d: soils treated using 60 W L^{-1}; e: soils treated using 100 W L^{-1}) (*m*/*z*177: C_{26-34} 17α25-norhopanes; *m*/*z*231: C_{26-28} TAS, in which, A. (20*S*)-C_{26} TAS, B. (20*R*)-C_{26} TAS and (20*S*)-C_{27} TAS, C. (20*R*)-C_{27} TAS, D. (20*S*)-C_{28} TAS, E. (20*R*)-C_{28} TAS; *m*/*z*245: C_{27-29} MTAS, in which, F. C_{27} 3-MTAS, G. C_{27} 4-MTAS, H. C_{29} 4-methyl-24-ethyl TAS, I. C_{29} 4,23,24-trimethyl TAS, J. C_{29} 3-methyl-24-ethyl TAS).

pany, USA). The mineral composition of the soils was analyzed using X-ray diffraction (XRD) (DMAX-2400, Rigaku Company, Japan).

2.4. Chemicals

Triton X-100 (chemically pure grade) and other solvents used (analytical reagent grade), 1,2,3,4-tetradeutero cholestane, and 1,2,3,4,5,6,7,8-octadeutero cholestane (spectroscopically pure grade) were supplied by Sinopharm Chemical (Beijing, China). Molecular formula of Triton X-100 in our study is $C_8H_{17}C_6H_4O(OCH_2CH_2)_{9.5}H$ with a molecular weight of 625, CMC of 0.31 mM, and Hydrophile Lipophile Balance of 13.5, respectively.

3. Results and discussion

3.1. Elution of super heavy oil

The concentrations of super heavy oil in eluted soils and Triton X-100 micellar solution are depicted in Fig. 1. The elution efficiency of Triton X-100 solution increased from 13.2% to 88.5% as the ultrasonic power density was increased from 0 to 100 W L^{-1}.

The relationship between the amount of super heavy oil that was dissolved or dispersed and the ultrasonic power density (illustrated in Fig. 1b) was similar to a first-order function:

$$-\ln\left(\frac{S_w}{S_0}\right) = 0.0264W + 0.0475R^2 = 0.9789 \quad (1)$$

in which W is the ultrasonic power density in W L^{-1}, S_0 is the amount in mg L^{-1} of oil dissolved or dispersed by Triton X-100 solution at a power density of 0 W L^{-1}, and S_w is the amount of oil dissolved or dispersed by Triton X-100 solution at the power density W in mg L^{-1}. S_w decreased with increasing power density. Possible reasons for this include interactions among various HOCs and competition between them for the same absorption site in soils [25], adsorption of HOCs and surfactant by soils, dissolution of HOCs by the water phase, adsorption of HOCs by surfactants adsorbed to the soil surface, dissolution HOCs in micelles [26], tilting and curling of HOCs adsorbed to the soil surface by ultrasound [3], and ultrasound enhancement of emulsification and dispersion of desorbed HOCs. The ultrasound also produced a 'smashing' effect on the bulk soil and suspended aggregates. This effect intensified with increasing ultrasonic power density and resulted in the continuous disruption of suspended aggregates [27].

In all of the experiments the concentration of Triton X-100 solution was 1.5 g L^{-1}, approximately 10 times its CMC (2.2×10^{-4} mol L^{-1}) [28]. Earlier investigators observed that at such high concentrations the main mechanism for eluting HOCs was solubilization [1,6,29]. Our results (Fig. 1b) indicated that the residual oil in eluted soils decreased with increasing ultrasonic power density according to the equation:

$$-\ln\left(\frac{C_w}{C_0}\right) = 0.4533W + 0.5439R^2 = 0.9627 \quad (2)$$

in which C_0 is the initial oil concentration in the AOCS in mg kg^{-1}, C_w is the oil concentration in mg kg^{-1} in soil eluted using a power density W, and W is the ultrasonic power density in W L^{-1}.

Interestingly, although Triton X-100 dissolved or dispersed super heavy oil followed the same trend as elution of oil by enhance ultrasound, the amount of the former only accounted for 24% of the total oil removed. Furthermore, this ratio decreased to 3% as the power density was increased to 100 W L^{-1} (Fig. 1a). Regardless of whether ultrasound was applied, a layer of oil accumulated at the water–soil interface after gravity separation for 24 h, which was different from light oil that formed an oil film at the surface of water [30]. The layer formed because the high concentration of oil (1.020 g cm^{-1}, more than that of water) and the AOCS (93.6 mg g^{-1}) resulted in multi-layer adsorption on the surface of the soil particles [3,6]. Increasing the power density increased the number of shock waves and enhanced cavitation processes, overcoming the interfacial forces between the soil particles and the surfactant [14,31,32], enabling the Triton X-100 micelles to easily infiltrate the soil particle surface [17] and promote detachment of the oil film absorbed in the outer soil layer. This oil films coagulated during the gravity sedimentation process into the layer observed at the water–soil interface.

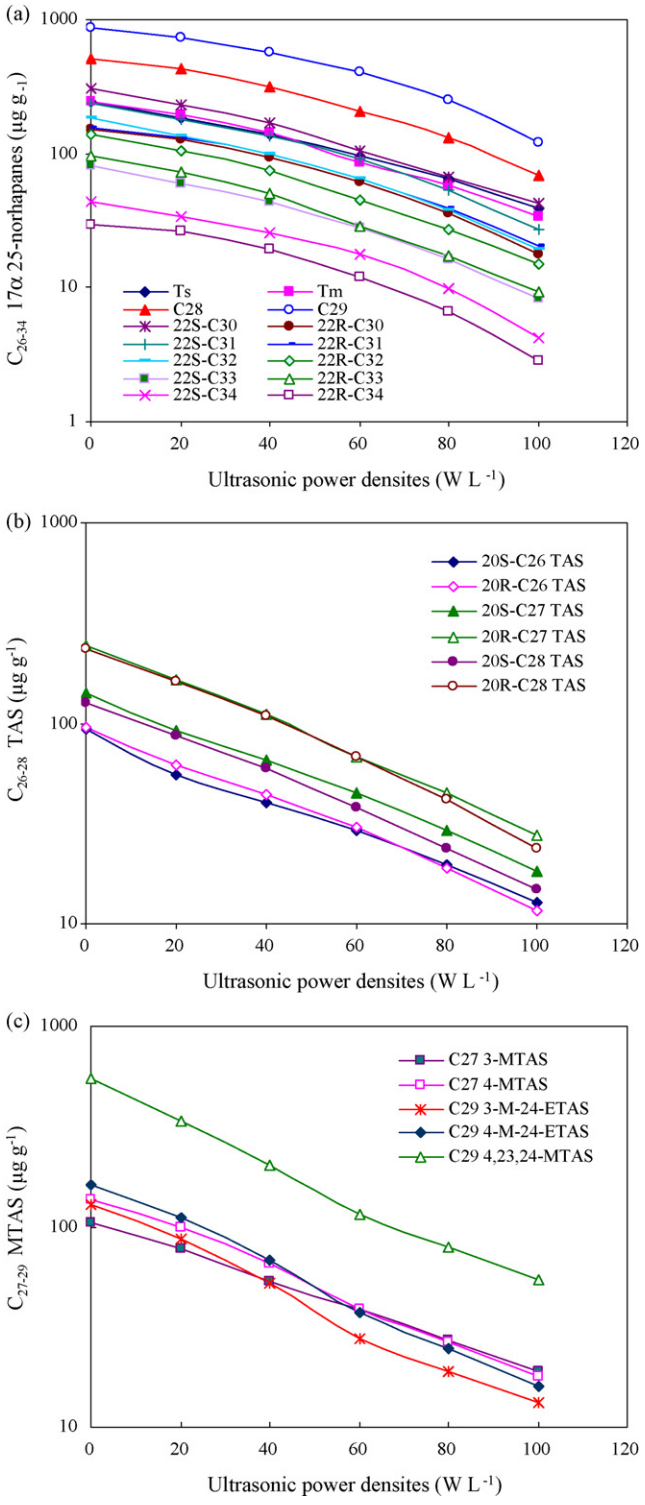

Fig. 3. Concentrations of 17α 25-norhopaness, TAS, and MTAS in the AOCS and eluted soils. (a: C_{26-34} 17α 25-norhopanes; b: C_{26-28} TAS; c: C_{27-29} MTAS).

3.2. Elution of biomarkers

3.2.1. Elution of 17α 25-norhopanes, TAS, and MTAS

The typical alkane biomarkers in the AOCS were the C_{26-34} 17α 25-norhopanes. They comprised 3.9% of the super heavy oil, with main peaks of C_{29} 17α 25-norhopane and C_{28} 17α 25-norhopane individually accounting for 1.0% and 0.6% of the super heavy oil (Figs. 2 and 3). The typical aromatic hydrocarbon biomarkers in the AOCS were C_{26-28} TAS and C_{27-29} MTAS, accounting for 1.1% and 1.2% of the super heavy oil. The (20*R*)-C_{27} TAS and 4,23,24-trimethyl triaromatic steroids (C_{29} 4,23,24-MTAS) were the main peaks for the C_{26-28} TAS and C_{27-29} MTAS homologs and accounted for 0.3% and 0.6% of the super heavy oil (Figs. 2 and 3).

Table 1
Ratios of 17α 25-norhopane, TAS, and MTAS in the AOCS and treated soils.

	22*S*/(22*S*+22*R*) C_{26-34} 17α 25-norhopanes	20*S*/(20*S*+20*R*) C_{26-28} TAS
AOCS	0.57	0.39
0 W L^{-1}	0.57	0.39
20 W L^{-1}	0.55	0.38
60 W L^{-1}	0.57	0.40
100 W L^{-1}	0.59	0.42

As the power density increased from 0 to 100 W L^{-1}, the average elution of C_{26-34} 17α 25-norhopanes increased from 13.3% to 88.7%. Elution of (22*S*)-C_{26} 17α 25-norhopane (the compound with the smallest carbon numbers) increased from 15.1% to 86.4%, whereas the elution of (22*R*)-C_{34} 17α25-norhopane (the compound with the greatest carbon numbers) increased from 10.5% to 91.4% (Figs. 2 and 3). As the power density increased from 0 to 100 W L^{-1}, the average elution of C_{26-28} TAS increased from 14.3% to 89.8%. Elution of (20*S*)-C_{26} TAS (the compound with the smallest carbon numbers) increased from 16.1% to 88.5%, and elution of (20*R*)-C_{28} TAS (the compound with the greatest carbon numbers) increased from 12.9% to 91.2% (Figs. 2 and 3). The average elution of C_{27-29} MTAS increased from 13.8% to 89.5% for the power density from 0 to 100 W L^{-1}, with the elution of C_{27} 3-MTAS (with the lowest carbon numbers) increasing from 17.1% to 84.9% and the elution of C_{29} 4,23,24-MTAS (with the greatest carbon numbers) increasing from 12.5% to 91.2% (Figs. 2 and 3). Thus, the elution trends of C_{26-34} 17α 25-norhopanes, TAS, and MTAS species with respect to power density was closely related to carbon numbers. A greater carbon numbers resulted in a larger improvement in elution when ultrasound was applied. A possible reason for this is that the use of ultrasound possibly reduces the hydration of the polyoxyethylene chains in Triton X-100 micellar solution [14,33], increasing the number of micelles [21] and ultimately increasing the elution of the three biomarkers. However, high-power ultrasound may also reduce the internal capacity of surfactant micellar vesicles and thus concentrate molecules containing greater C atoms or of greater polarity in the outer portion of the micelles [14,33]. In addition, for a hydrocarbon, the more C and the stronger polarity, it is easier to be absorbed by polar species, such as asphalt [34,35], and is more easily dislodged from the soil surface by ultrasound [35], as in the case of 17α 25-norhopanes, TAS, and MTAS homologs containing a greater carbon numbers.

3.2.2. Residual 17α 25-norhopane and TAS in eluted soils

The relative amounts of the 22*S*/(22*S*+22*R*) of C_{26-34} 17α 25-norhopanes and 20*S*/(20*S*+20*R*) of C_{26-28} TAS extracted at a power level of 20 W L^{-1} were lower than those in the AOCS and treated soils in the absence of ultrasound (Table 1), indicating that ultrasound at low power density preferentially eluted (*S*)-17α 25-norhopanes and TAS by Triton X-100 micellar solution. Possible reasons for this are that the *R* stereoisomer is the biological configuration, while the *S* stereoisomers have been converted geologically [36–38]. Both the stabilization and the polarity of the *S*-configured molecules are weaker than *R*-configured molecules. In addition, ultrasound at a power density of 20 W L^{-1} displayed a weak ability to dislodge and emulsify biomarkers adsorbed to the soil surface [14,39], which benefits weak hydrophobic organic to dissolve in the inner of surfactant micelle [36], and thus low power density enhanced the dissolved elution of *S*-shaped biomarker with the

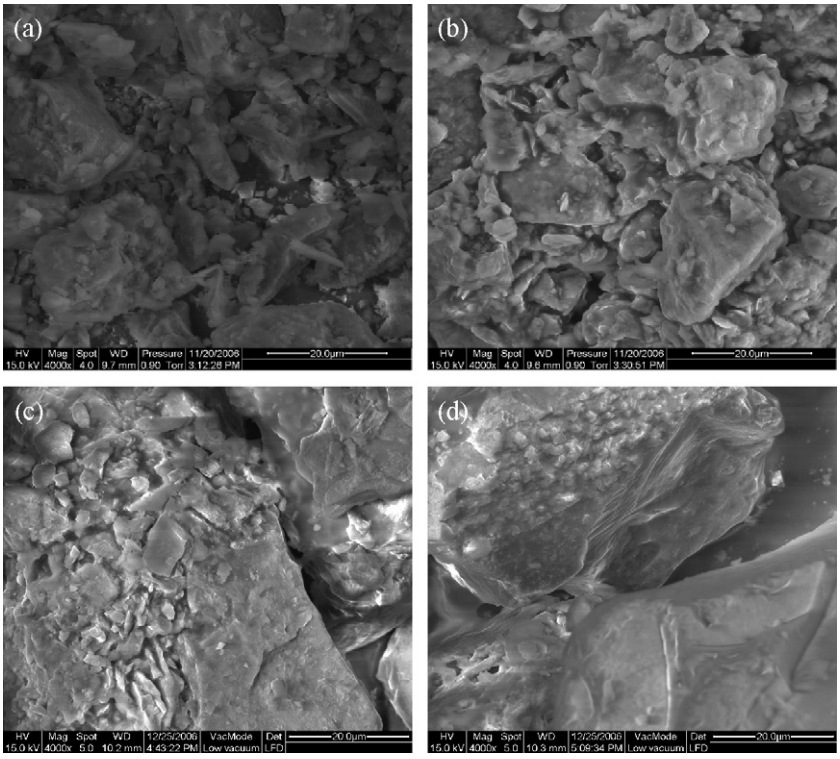

Fig. 4. SEM image depicting the surfaces of soil particles. (a: Clean soil; b: AOCS; c: eluted soil at 20 W L^{-1}; d: eluted soil at 100 W L^{-1}).

characteristics of stable chemical property and weak hydrophobicity.

The two ratios, 22*S*/(22*S* + 22*R*) of C_{26-34} 17α 25-norhopanes and 20*S*/(20*S* + 20*R*) of C_{26-28} TAS, increased with increasing power density from 20 to 100 W L^{-1} (Table 1). This may be due to stronger hydrophobicity of *S*- than that of *R*-biomarkers [36,37,40]. Thus, the elution of *S*-biomarkers followed the same trend as C_{26-34} 17α25-norhopane and C_{26-28} TAS containing fewer C atoms, whereas the elution of *R*-biomarkers followed the same trend as C_{26-34} 17α5-norhopanes C_{26-28} TAS containing greater C atoms.

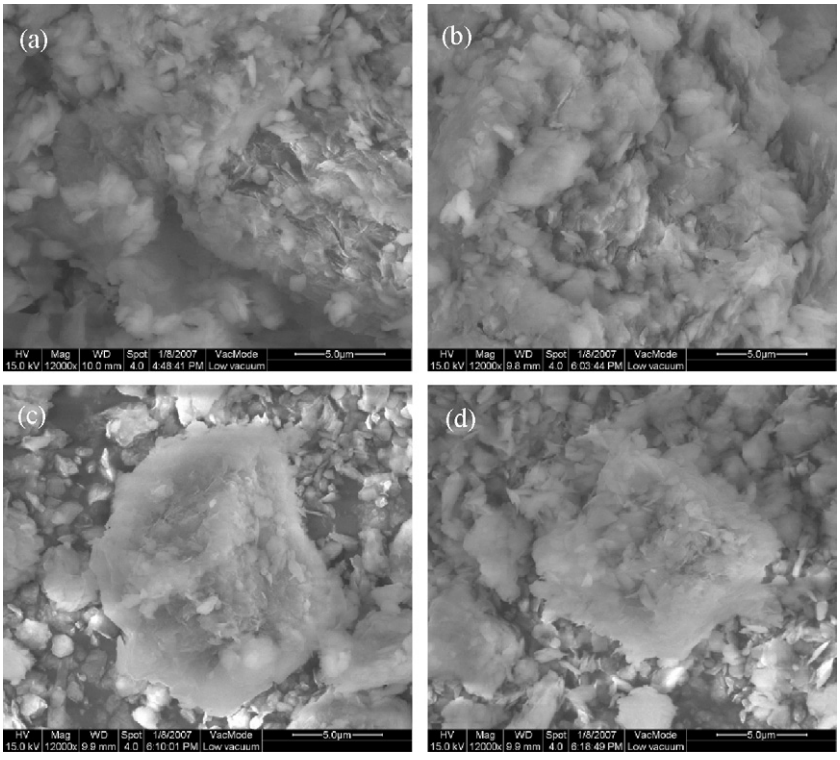

Fig. 5. SEM image of solid particles suspended in Triton X-100 solution (a: 0 W L^{-1}; b: 20 W L^{-1}; c: 60 W L^{-1}; d: 100 W L^{-1}).

3.3. Surface characteristics of clean soils, the AOCS, and eluted soils

Fig. 4 contains a series of SEM images depicting the surfaces of soil particles. The soil surface was composed of a variety of clay, silt, and sand particles. However, the AOCS was mainly composed of soil aggregates with a particle size of approximately 60 μm, which is very different from clean soils (Fig. 4). Other authors have provided similar descriptions [41]. This may be due to the heavy oil first adsorbing to the surface of smaller particles such as clay and silt, followed by aggregation into larger granules with a high oil concentration. These granules then stick to sand particles of relatively larger size, forming the aggregates comprising the surface of the AOCS.

Following treatment with ultrasound at 20 W L^{-1}, most of the residual super heavy oil present in the soils was detached from the surface and 40% of the soil surface area was in the form of "bare patches". This figure reached almost 80% when the power density of the ultrasound was increased to 100 W L^{-1} (Fig. 4). These observations demonstrate that ultrasound at high power densities is helpful in eluting super heavy oil and its biomarkers from the AOCS.

3.4. Morphology of suspended solid in Triton X-100 micellar solution

Fig. 5 contains SEM images of solid particles suspended in Triton X-100 solution. Without ultrasound, the suspended solids were mainly composed of aggregates larger than 30 μm in size. Although there were some small particles approximately 1–3 μm in size, almost all of them were bound to large aggregates, and they rarely existed in the free state (Fig. 5), because the surfactant micelles (or vesicles) assisted the HOCs in coagulating and forming aggregates [42]. Furthermore, the Ca^{2+} and Mg^{2+} ions in soil minerals enabled non-ionic surfactant micelles (or vesicles) to easily form larger aggregates [10,11].

There was almost no difference in the morphology and size of suspended particles between samples treated without ultrasound and those treated using a power density of 20 W L^{-1} (Fig. 5). This is due to that the low-power ultrasound produced only a weak dispersion effect on HOCs [14,39]. When the power density of the ultrasound was increased to 60 W L^{-1}, the largest diameter of suspended aggregates decreased to 15 μm, and a large number of small particles with sizes between 1 and 3 μm were observed. When the power density was increased to 100 W L^{-1}, the largest particle diameter decreased to 12 μm. Possible reasons for this are that the dispersion ability of the ultrasound was directly related to the power density. High power density resulted in increased dispersion that ultimately produced smaller diameter aggregates and a more stable colloid system [39]. In addition, higher ultrasonic power density increased the negative potential on the surface of the suspended aggregates [40], resulting in a greater repulsive force between the particles.

3.5. Mineral and elemental composition of clean soils, the AOCS, and eluted soils

Analysis by X-ray diffraction revealed that the primary minerals present in the clean and eluted soils were quartz (SiO_2) and feldspar ($CaAl_2Si_2O_8$), combined with lesser amounts of muscovite ($KAl_2(Al{\cdot}Si_3O_{10})(OH)_2$) and chlorite ($(Mg,Al,Fe)_6[(Si,Al)_4O_{10}](OH)_8$) (Fig. 6). The relative abundance of clay minerals such as chlorite and muscovite in eluted soils decreased with increasing ultrasonic power densities, which agreed with the increasing proportion of small particles (1–3 μm) observed using SEM (Figs. 4 and 5). The relative abundance of

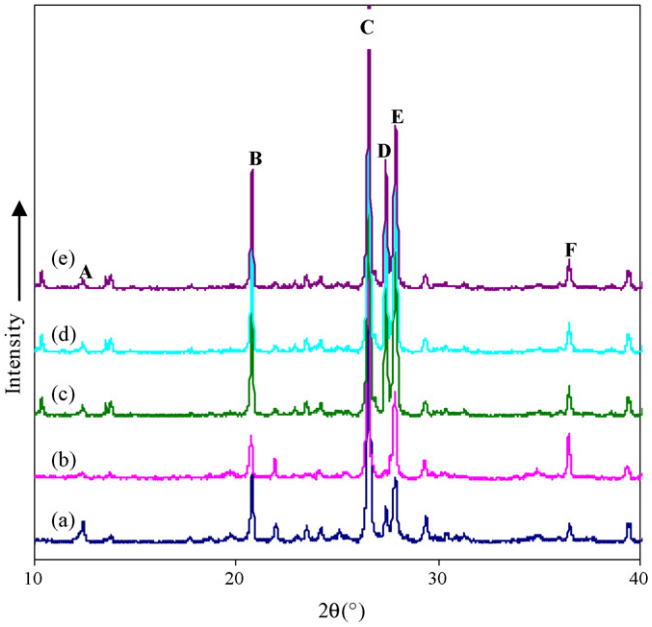

Fig. 6. XRD plots for clean and eluted soil. (a: Clean soils; b: soil eluted using 0 W L^{-1}; c: soil eluted using 20 W L^{-1}; d: soil eluted using 60 W L^{-1}; e: soil eluted using 100 W L^{-1}). (A: Chlorite $(Mg,Al,Fe)_6[(Si,Al)_4O_{10}](OH)_8$; B: Quartz; C: Quartz and $KMg_3Si_3AlO_{10}F_2$; D: Feldspar; E: Muscovite; F: Feldspar).

Ca, Mg, and Al in the eluted soils also decreased with increasing power density (Fig. 7). Ca, Mg, and Al are the main constituents of the secondary minerals chlorite and muscovite [11], which decreased upon dispersion and suspension. In addition, Triton X-100 easily underwent association reactions with the Ca^{2+} and Mg^{2+} in feldspar and muscovite [9,43]. Increased ultrasonic power density also improved the dispersion of Ca^{2+} and Mg^{2+} ions in the Triton X-100 solution [10].

3.6. Functional groups

FT-Raman spectra of functional groups appearing in eluted soils are depicted in Fig. 8. The absorption bands of eluted soils were mainly present at 3700–3100, 3000–2800, 1643, 1462, 1310–950, and 783 cm^{-1}. A prominent mound-shaped absorption peak appeared between 3700–3100 cm^{-1} and was attributed to –OH, $–NH_2$, –COOH, and carbonyl groups that easily form hydrogen bonds [11]. The intensity of this peak decreased with increasing power density, indicating that the increased ultrasonic power improved the elution of hydrogen-bonded oil components in the form of colloids and asphalts.

Absorption peaks appearing between 3000 and 2800 cm^{-1} and at 1462 cm^{-1} were assigned to stretching vibrations of $–CH_3$ and $–CH_2$ in aliphatic chains, and the intensity of these peaks represented the abundance of aliphatic compounds [44]. The intensity of these two absorption peaks decreased with increasing power density, indicating that increased ultrasonic power densities improved the elution of aliphatic compounds. This matched the elution profile observed for $C_{26–34}$ 17α 25-norhopane (as shown in Figs. 2 and 3).

The peak located at 1643 cm^{-1} was assigned to stretching vibrations of aromatic rings, heterocyclic rings, and –NHR groups adjacent to aromatic structures. This peak reflected the abundance of aromatic compounds [11]. The intensity of the peak decreased with increasing power density, indicating that increased power improved the removal of aromatic components of the oil. This was similar to the results obtained for TAS and MTAS (Figs. 2 and 3).

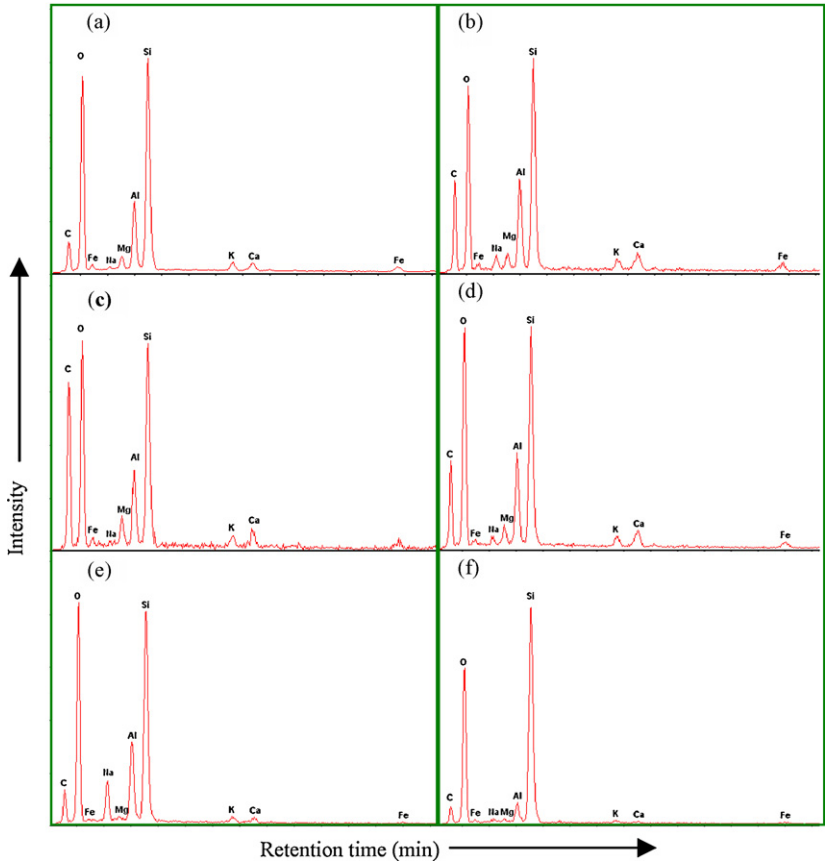

Fig. 7. Energy spectra of soil particle surfaces. (a: Clean soil, b: AOCS, c: soil eluted using 0 W L^{-1}; d: soil eluted using 20 W L^{-1}; e: soil eluted using 60 W L^{-1}; f: soil eluted using 100 W L^{-1}).

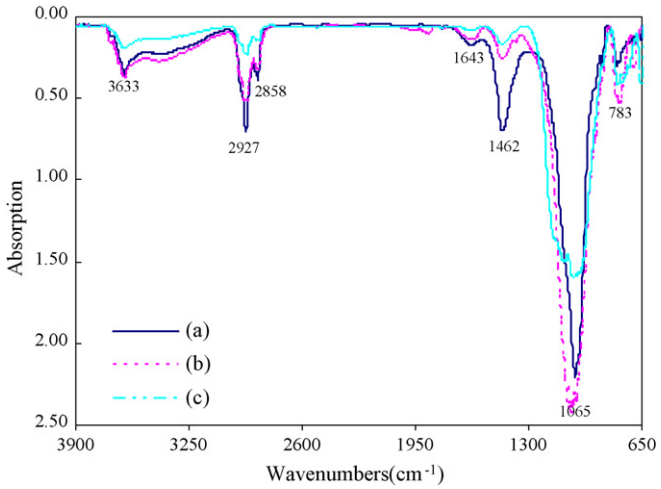

Fig. 8. FT-Raman spectra of functional groups appearing in eluted soils. (a: Soil eluted using 0 W L^{-1}; b: soil eluted using 20 W L^{-1}; c: soil eluted using 100 W L^{-1}).

The O–Si–O stretching vibration appeared as a broad peak between 1310 and 950 cm^{-1}. The intensity of this peak increased with increasing power density, in agreement with SEM observations and measurements of elemental composition.

4. Conclusions

(1) The concentration of residual super heavy oil and related biomarkers in treated soils decreased in a similar first-order manner with respect to increased ultrasound power density.

(2) The elution trends of C_{26-34} 17α 25-norhopanes, C_{26-28} TAS, and C_{27-29} MTAS compounds were closely related to carbon numbers regardless of whether ultrasound was applied.

(3) The application of ultrasound at power densities of 20–100 W L^{-1} was helpful to the elution of (22*R*)-C_{26-34} 17α 25-norhopanes and (20*R*)-C_{26-28} TAS. Ultrasound at power levels greater than 60 W L^{-1} reduced the level of organic functional groups present in the treated soil samples and represents a potentially useful method for enhancing the removal of super heavy oil from contaminated soil.

Acknowledgement

This study was funded by two grants from the National Natural Science Foundation of China (no. 40772146).

References

[1] G.D. Ji, T.H. Sun, J.R. Ni, Surface flow constructed wetland for heavy oil-produced water treatment, Bioresour. Technol. 98 (2007) 436–441.
[2] G.D. Ji, T.H. Sun, J.R. Ni, J.J. Tong, Anaerobic baffled reactor (ABR) for treating heavy oil produced water with high concentrations of salt and poor nutrient, Bioresour. Technol. 100 (2009) 1108–1114.
[3] X. Song, L.H. Zhang, G.D. Ji, Study on ultrasonic disingegration of heay oil polluted clay granule, Chin. J. Environ. Eng. 3 (2009) 363–366.
[4] G.D. Ji, Y.S. Yang, Q.X. Zhou, Phytodegradation of extra heavy oil-based drill cuttings using mature reed wetland: an in situ pilot study, Environ. Int. (2004) 509–517.
[5] F.I. Khan, T. Husain, R. Hejazi, An overview and analysis of site remediation technologies, J. Environ. Manage. 71 (2004) 95–122.
[6] G.D. Ji, G.H. Zhou, Remediation of soil contaminated with oil pollutants by ex-situ chemical washing, Acta Scientiarum Naturalium Universitatis Pekinensis 43 (2007) 863–871.
[7] A. Martin, Ageing, bioavailability, and overestimation of risk from environment pollutants, Environ. Sci. Technol. 34 (2000) 4259–4265.

[8] G.D. Ji, G.H. Zhou, A technology for remedying aging heavy oil polluted soils using eluting solution, Patent of invention of China, ZL200610152986.X (2006).
[9] K. Yang, L.Z. Zhu, B.S. Xing, Sorption of sodium dodecylbenzene sulfonate by montmorillonite, Environ. Pollut. 145 (2007) 571–576.
[10] Z. Masliyah, Z. Zhou, J. Xu, Understanding water-based bitumen extraction from Athabasca oil sands, Can. J. Chem. Eng. 82 (2004) 628–654.
[11] D.V. Trong, R. Jhaa, S.Y. Wua, Wettability determination of solids isolated from oil sands, Colloids Surf. A: Physicochem. Eng. Aspects 337 (2009) 80–90.
[12] P. Wang, A.A. Keller, Particle-size dependent sorption and desorption of pesticides within a water–soil–nonionic surfactant system, Environ. Sci. Technol. 42 (2008) 3381–3387.
[13] K. Yang, L.Z. Zhu, B.S. Xing, Enhanced soil washing of phenanthrene by mixed solutions of Trition X-100 and SDBS, Environ. Sci. Technol. 40 (2006) 4274–4280.
[14] D. Feng, C. Aldrich, Sonochemical treatment of simulated soil contaminated with diesel, Adv. Environ. Res. 4 (2000) 103–112.
[15] A.P. Newman, J.P. Lorimer, An investigation into the ultrasonic treatment of polluted solids, Ultrason. Sonochem. 4 (1997) 153–156.
[16] D. Feng, C. Aldrich, Ex-situ diesel contaminated soil washing with mechanical methods, Miner. Eng. 9 (2001) 1093–1100.
[17] Y.U. Kim, M.C. Wang, Effect of ultrasound on oil removal from soils, Ultrasonics 41 (2003) 539–542.
[18] J. Timothy, A.C. Mason, A. Sumel, Sonic and ultrasonic removal of chemical contaminants from soil in the laboratory and on a large scale, Ultrason. Sonochem. 11 (2004) 205–210.
[19] R. Kamalavathany, Analysis and modeling of ultrasound enhanced soil washing process, New Jersey Institute of Technology, New Jersey, 1997.
[20] T.J. Mason, A. Collings, A. Sumel, Sonic and ultrasonic removal of chemical contaminants from soil in the laboratory and on a large scale, Ultrason. Sonochem. 11 (2004) 205–210.
[21] K. Urum, T. Pekdemir, D. Ross, S. Grigson, Crude oil contaminated soil washing in air sparging assisted stirred tank reactor using biosurfactants, Chemosphere 60 (2005) 334–343.
[22] A.P. Schwab, J. Su, S. Wetzel, et al., Extraction of petroleum hydrocarbons from soil by mechanical shaking, Environ. Sci. Technol. 33 (1999) 1940–1945.
[23] B. Bennett, M. Fustic, P. Farrimond, H. Huang, S.R. Larter, 25-Norhopanes: formation during biodegradation of petroleum in the subsurface, Org. Geochem. 37 (2006) 787–797.
[24] J.P. Bao, C.S. Zhu, Impacts of biodegradation on composition and maturity of aromatic hydrocarbons, Sci. China Ser. D: Earth Sci. 38 (2008) 55–63.
[25] R. Khalladi, O. Benhabiles, F. Bentahar, N. Moulai-Mostefa, Surfactant remediation of diesel fuel polluted soil, J. Hazard. Mater. 164 (2009) 1179–1184.
[26] S. Laha, B. Tansel, U. Achara, Surfactant–soil interactions during surfactant-amended remediation of contaminated soils by hydrophobic organic compounds: a review, J. Environ. Manage. 90 (2009) 95–100.
[27] R.S. Juang, S.H. Lin, C.H. Cheng, Liquid-phase adsorption and desorption of phenol onto activated carbons with ultrasound, Ultrason. Sonochem. 13 (2006) 251–260.
[28] Z.N. He, Studies on Washing High Oil Contaminated Soil, Peking University, 2005.
[29] M.C. Chang, C.R. Huang, S.Y. Shu, Effects of surfactants on extraction of phenanthrene in spiked sand, Chemosphere 41 (2000) 1295–1300.
[30] M. Han, G.D. Ji, J.R. Ni, Washing of field weathered crude oil contaminated soil with an environmentally compatible surfactant, alkyl polyglucoside, Chemosphere 76 (2009) 579–726.
[31] H Kyllonen, P. Pirkonen, V. Hintikka, Ultrasonically aided mineral processing technique for remediation of soil contaminated by heavy metals, Ultrason. Sonochem. 11 (2004) 211–216.
[32] Y.J. Wang, F. Cannon, Mechanisms of advanced oxidation processing on bentonite consumption reduction in foundry, Environ. Sci. Technol. 39 (2005) 7712–7718.
[33] B. Bennett, S. Larter, L. Carbognani, P. Pereira-Almao, Identification and characterization of reaction proxies for monitoring the progress of thermal processing of heavy oils and tar sands under vis-breaking conditions, Energy Fuels 22 (2008) 440–448.
[34] G.D. Ji, T.H. Sun, Q.X. Zhou, X. Sui, S.J. Chang, P.J. Li, Constructed subsurface flow wetland for treating heavy oil-produced water of the Liaohe Oilfield in China, Ecol. Eng. 18 (2002) 459–465.
[35] C. Zhou, Ultrasound-Enhanced Washing Using for Remediation of Heavy Oil-polluted Soil, Master thesis, Peking University, Beijing, 2009.
[36] P. Boehm, Resolving the origin of the petrogenic hydrocarbon background in Prince William Sound, Alaska, Environ. Sci. Technol. 35 (2001) 471–479.
[37] M. Ian, D. Head, J. Martin, S.R. Larter, Biological activity in the deep subsurface and the origin of heavy oil, Nature 426 (2003) 344–352.
[38] J.B. Jochen, D.L. Gordon, E.S. Roger, Biomarker evidence for green and purple sulphur bacteria in a stratified Palaeoproterozoic sea, Nature 437 (2005) 866–870.
[39] T. Pekdemir, M.C. Opur, K. Urum, Emulsification of crude oil-water systems using biosurfactants, PSEP 83 (2005) 38–46.
[40] Y.E. Wang, S.H. Deng, C.M. Yang, K.H. Zhou, Studies on reducing viscosity of crude oil using ultrasound-surfactant, Acoustics Technol. 20 (2001) 149–151.
[41] M.J. Mann, Full-scale and pilot-scale soil washing, J. Hazard. Mater. 66 (1999) 119–136.
[42] P. Conte, A. Agretto, R. Spaccini, Soil remediation: humic acids as natural surfactants in the washings of highly contaminated soils, Environ. Pollut. 135 (2005) 515–522.
[43] M.J. Sanchez-Martın, M.C. Dorado, C.D. Hoyo, M.S. Rodrĭguez-Cruz, Influence of clay mineral structure and surfactant nature on the adsorption capacity of surfactants by clays, J. Hazard. Mater. 150 (2008) 115–123.
[44] B.D. Sparks, L.S. Kotlyar, J.B.O. Carroll, K.H. Chung, Athabasca oil sands: effect of organic coated solids on bitumen recovery and quality, Petrol. Sci. Eng. 39 (2003) 417–430.